INTERNATIONAL JOURNAL OF
NUMERICAL ANALYSIS AND MODELING
Volume 19, Number 2-3, Pages 329–346

A COMPARISON OF REGULARIZATION METHODS FOR BOUNDARY OPTIMAL CONTROL PROBLEMS

GIORGIO BORNIA, ANDREA CHIERICI, AND SAIKANTH RATNAVALE

Abstract. In this work we propose and compare multiple approaches for the formulation of boundary optimal control problems constrained by PDEs. In particular, we define a property of balanced regularity that is not satisfied by traditional approaches. In order to instead guarantee this property, we consider the use of other regularization terms, one involving fractional Sobolev norms and the other one based on the introduction of lifting functions. As required by the fractional norm approach, we present a semi-analytical numerical implementation of the fractional Laplacian operator. All the proposed formulations are also considered in conjunction with constraints of inequality type on the control variable. Numerical results are reported to compare all the presented regularization techniques.

Key words. Boundary optimal control, regularization methods, inequality constraints.

1. Introduction

Boundary optimal control problems are one of the most interesting classes of optimal control problems constrained by partial differential equations. In fact, the possibility of controlling the behavior of a physical system often takes place only by changing the values of certain quantities on the boundary of its domain, especially when the interior of the physical system is not accessible or no physical mechanism can be triggered inside the domain from the outside. Many works have been published both on the mathematical analysis (see [1, 2]) and the numerical approximation (see [3] and references therein) of this class of problems.

In this work we turn our attention to the mathematical formulation of boundary optimal control problems and how it affects the function space setting of optimal states and controls. Fundamental results about Sobolev spaces imply that the connection between functions defined on the domain of a PDE and their restriction to the boundary gives rise to the occurrence of *fractional-indexed* Sobolev spaces. In the context of boundary optimal control, this may lead to the presence of fractional norms and consequently fractional derivatives in the first-order necessary conditions that characterize optimal solutions.

Due to the challenges in the numerical approximation of fractional derivatives, simple optimal control techniques have been traditionally chosen in order to circumvent their presence. In many works, the control problem is simplified by resorting to integer-indexed Sobolev spaces (e.g., H^1 controls instead of $H^{1/2}$ controls). This approach features the drawback of a more restrictive control space than the natural space that is dictated by the range of the trace operator. In order to overcome this restriction, still without involving fractional norms, an approach based on the concept of lifting functions has been studied in the literature [4, 5, 6, 7].

To the best of our knowledge, the present work is a first attempt at encompassing multiple boundary control approaches in a unified view. In particular, the

Received by the editors September 10, 2021 and, in revised form, January 3, 2022.
2000 *Mathematics Subject Classification.* 49N60, 49M25, 35R11.

traditional integer-indexed approach, which is placing unnecessary restrictions on the function spaces, is compared to two formulations that bypass such limits: on one hand, the lifting function formulation; on the other, a direct approach based on a numerical approximation of the fractional Laplacian.

Fractional operators on bounded domains (and, in particular, the fractional Laplacian) can be seen as nonlocal diffusion operators [8]. For this reason, the numerical implementation of these operators is not straightforward and represents a topic of increasing interest in the scientific community. Many works have been recently published on this subject, and the interested reader can consult [9, 10]. Moreover, several articles including comparisons of the different fractional Laplacians have appeared recently, see [11, 12, 13]. A common approach for the numerical simulation of the fractional Laplacian, called spectral fractional Laplacian, is based on the Dunford-Taylor method. In particular, a direct approximation of the inverse of the fractional operator can be obtained through the so-called Balakrishnan formula and a sinc quadrature scheme. Even though this technique does not allow a direct implementation of the operator, it is advantageous from the point of view of the computational costs and the ease of implementation. The interested reader can consult [14, 15]. A different technique based on the Dunford-Taylor method, and usually called integral fractional Laplacian, can be defined using the Fourier transform. Similarly to the spectral fractional Laplacian, it relies on a sinc quadrature scheme. However, this approach allows the numerical representation of the fractional operator, instead of its inverse. The interested reader can consult [16] and references therein. Lastly, the direct numerical implementation of the real-space formula for the fractional Laplacian can be performed. This approach is known as Riesz fractional Laplacian and can be traced back to the nonlocal numerical simulations [17].

In this paper, we apply the Riesz approach to implement and test the fractional Laplacian operator in a finite element framework. Usually, a standard technique used for nonlocal simulations, including the Riesz fractional Laplacian implementations, provides the limitation of the interactions to a ball of radius $\lambda > 0$. This approach allows to reduce the computational costs and the sparsity pattern of the interaction matrix. However, this technique poses many challenges, e.g. the prescription of nonlocal analogues of boundary conditions and the uncertainty and sparsity of model parameters and data. The interested reader can consult [18, 19, 20, 21]. In this work, we introduce a semi-analytical technique for a direct implementation of the double integral, without any limitation on the interaction domain.

Outline of the paper. In the next Section, we introduce a class of boundary optimal control problems with particular attention to the regularization term. We present the definition of balanced regularity and consider different regularization techniques in terms of how they behave with respect to this property. These lead to different optimality systems for the proposed techniques that are presented in Section 3. Since the fractional optimal control problem gives rise to fractional operators, in Section 4 we introduce a numerical implementation of the fractional Laplacian operator. The addition of control inequality constraints is described in Section 5. Lastly, Section 6 is devoted to presenting some numerical results to compare all the proposed optimal control problems for both two- and three-dimensional simulations.

2. Boundary optimal control problems and balanced regularity

In this section, we introduce a class of boundary optimal control problems and we define the property of balanced regularity that naturally arises with them. Only to keep the exposition simple, we describe these features with a model problem given by a Laplace constraint operator, Dirichlet boundary conditions, and a tracking-type cost functional. We remark that the issues we will be highlighting are also encountered in boundary optimal control problems with general PDE constraints, boundary conditions other than Dirichlet (such as Neumann or Robin), and cost functionals of non-tracking type.

Let us first recall some basic definitions for the symbols that will be used in the following. Let Ω be a bounded domain with boundary $\partial\Omega$ and unit normal vector field $\mathbf{n}$. For any domain $\mathcal{O} \subseteq \Omega$, we denote with $H^m(\mathcal{O})$ the classical Sobolev space of order m. For any $\Gamma \subset \partial\mathcal{O}$, we denote with γ_0 and γ_1 the operators

$$\gamma_0 \,:\, H^m(\mathcal{O}) \to H^{m-1/2}(\Gamma) \tag{1}$$

$$\gamma_1 \,:\, H^m(\mathcal{O}) \to H^{m-3/2}(\Gamma) \tag{2}$$

corresponding to the trace of a function on Γ and the trace of the normal derivative of a function on Γ, respectively. These operator is surjective [22]. Also, for any boundary portion $\Gamma \subseteq \partial\mathcal{O}$, we use the notation $H^1(\mathcal{O};\Gamma)$ for functions $H^1(\mathcal{O})$ with zero trace on Γ. When $\Gamma = \partial\mathcal{O}$, we also use the notation $H^1_0(\mathcal{O}) = H^1(\mathcal{O};\partial\mathcal{O})$. The symbols ∇_Γ and Δ_Γ denote the surface gradient and surface Laplacian on $\partial\Omega$, respectively. In the rest of the paper, the inner product over $H^m(\mathcal{O})$ is denoted by $(f,g)_m$, whenever m is a non-negative integer. We define, for $f\,g \in L^1(\mathcal{O})$ and $\boldsymbol{u}\cdot\boldsymbol{v} \in L^1(\mathcal{O})$,

$$(f,g)_{\mathcal{O}} = \int_{\mathcal{O}} f g d\boldsymbol{x}\,, \qquad (\boldsymbol{u},\boldsymbol{v})_{\mathcal{O}} = \int_{\mathcal{O}} \boldsymbol{u}\cdot\boldsymbol{v} d\boldsymbol{x}\,.$$

We will neglect the domain label when $\mathcal{O} \equiv \Omega$.

In order to describe the notion of *balanced regularity*, we now introduce a class of model Dirichlet boundary optimal control problems. We denote the control boundary as $\Gamma_c \subseteq \partial\Omega$. On Γ_c, Dirichlet optimal conditions are sought.

Problem 1. *Find a state-control pair $(u,q) \in H^1(\Omega)\times Q$ which minimizes the cost functional*

$$\mathcal{J}(u,q) = \frac{1}{2}\|u-u_d\|^2_{L^2(\Omega_d)} + \frac{\alpha}{2}G(q)^2\,, \tag{3}$$

under the constraints

$$\Delta u = 0 \qquad \text{on } \Omega\,, \tag{4}$$

$$u = q \qquad \text{on } \Gamma_c\,, \tag{5}$$

$$u = 0 \qquad \text{on } \partial\Omega \setminus \Gamma_c\,. \tag{6}$$

The functional $G(q)$ is a given regularization term and it is multiplied by a constant $\alpha > 0$. In the following, various choices of the functional $G(q)$ will be considered, for all of which the existence of a minimizer is well-established [23]. The desired state function u_d is also given, and it may be intended to be achieved on a subset $\Omega_d \subseteq \Omega$. Moreover, Q is a Hilbert space on the domain Γ_c, depending on the choice of the functional $G(q)$ in (3) and on the Dirichlet boundary conditions in (5), that can be more precisely written using the trace operator as $\gamma_0 u = q$

on Γ_c. This immediately shows that, while $H^1(\Omega)$ is the space for the optimal states, the natural space where optimal boundary controls q should be sought is $Q = H^{1/2}(\Gamma_c)$, as dictated by the range of the trace operator (1). Thus, we can propose the following definition.

Definition 1. *An optimal control problem is said to have the* balanced regularity *property if the optimal states belong to the Sobolev spaces $H^a(\Omega)$ with differentiability index a, while the boundary optimal controls belong to the Sobolev spaces $H^b(\Gamma)$ with differentiability index $b = a - \frac{1}{2}$, as dictated by the range of the trace operator.*

A problem that possesses the balanced regularity property will search for controls in the largest trace space without additional restrictions. In general, the regularization functional $G(q)$ can be chosen in multiple ways.

$H^1(\Gamma_c)$ approach. The Sobolev space $H^1(\Gamma_c)$ is the largest integer-indexed Sobolev space contained in $H^{1/2}(\Gamma_c)$. Thus, a simple and immediate choice of $G(q)$ that guarantees the existence of a minimizer is

$$G(q) = \|q\|_{H^1(\Gamma_c)}\,.$$

In literature, many works use this approach to deal with boundary controls. However, as noted above, in this case the control space is more restrictive than the natural one and the balanced regularity property is not satisfied.

$H^{1/2}(\Gamma_c)$ approach. As noted above, this is the most natural choice of $G(q)$ in (3) that guarantees the existence of a boundary optimal control. In particular, we impose

$$G(q) = \|q\|_{H^{1/2}(\Gamma_c)}\,. \tag{7}$$

The balanced regularity property is then clearly satisfied for this problem. The drawback of this approach is that the differentiation of the fractional norm on q induces an optimality system that contains the fractional derivatives of q, and the numerical discretization of fractional derivatives poses considerable difficulties with respect to standard derivatives.

$H^1(\Omega_c)$ approach (lifting). This formulation is inspired by the method of reduction to homogeneous boundary conditions. We consider an arbitrary domain $\Omega_c \subseteq \Omega$, such that $\Gamma_c \subset \partial\Omega_c$. Then, we can decompose the state u as $u = \hat{u} + \tilde{q}$, with $\hat{u} = 0$ on $\partial\Omega$. In this case the control space can be defined as

$$Q = \{\tilde{q} \in H^1(\Omega) \text{ such that } \tilde{q} = 0 \text{ in } \Omega \setminus \Omega_c \text{ and } \gamma_0(\tilde{q}) = 0 \text{ on } \partial\Omega_c \setminus \Gamma_c\}\,.$$

This problem results in a reformulation of the control Problem 1.

Problem 2. *Find a state-control pair $(\hat{u}, \tilde{q}) \in H^1(\Omega) \times Q$ which minimizes the cost functional*

$$\mathcal{J}(\hat{u}, \tilde{q}) = \frac{1}{2}\|\hat{u} + \tilde{q} - u_d\|^2_{L^2(\Omega_d)} + \frac{\alpha}{2}\|\tilde{q}\|^2_{H^1(\Omega_c)}\,,$$

under the constraints

$$\begin{aligned} &\Delta(\hat{u} + \tilde{q}) = 0 && \text{on } \Omega\,,\\ &\hat{u} = 0 && \text{on } \partial\Omega\,. \end{aligned}$$

Thus, this method consists of a distributed control approach, where the optimal Dirichlet boundary control is obtained via trace restriction as $\gamma_0(u) = \gamma_0(\hat{u} + \tilde{q}) = \gamma_0(\tilde{q})$. In this way, the boundary controls belong to the natural trace space.

3. First-order necessary conditions and optimality systems

The formal Lagrange method is used to derive the first-order necessary conditions and the optimality systems. For additional details, see [24]. The solution of the optimality systems arising as first-order necessary conditions for the proposed optimal control problems yields candidate optimal solutions.

$H^1(\Gamma_c)$ control. We define the Lagrange functional for the standard Dirichlet problem without inequality constraints as

$$\mathcal{L}(u,q,\lambda_1,\lambda_2) = \frac{1}{2}\int_{\Omega_d} |u-u_d|^2\,d\Omega + \frac{\alpha}{2}\left(\int_{\Gamma_c} q^2\,dS + \int_{\Gamma_c} |\nabla q|^2\,dS\right) - \int_{\Omega} \lambda_1(-\Delta u)\,d\Omega - \int_{\Gamma_c} \lambda_2(u-q)\,dS\,.$$

Here, λ_1 and λ_2 are Lagrangian multipliers defined on Ω and Γ_c respectively. By setting $\lambda = \lambda_1$ and $\lambda_2 = -\gamma_1(\lambda)$, the optimality system for all variations $\delta u \in H^1(\Omega;\partial\Omega \setminus \Gamma_c)$, $\delta q \in H^1(\Gamma_c)$ and $\delta\lambda \in H^1(\Omega;\partial\Omega)$ is given by the adjoint, control, state equations with the boundary conditions as below.

$$\begin{aligned}
&((u-u_d),\delta u)_{\Omega_d} - (\nabla\lambda,\nabla(\delta u))_{\Omega} + \left(\frac{\partial\lambda}{\partial n},\delta u\right)_{\Gamma_c} = 0\,,\\
&\alpha[(q,\delta q)_{\Gamma_c} + (\nabla q,\nabla(\delta q))_{\Gamma_c}] - \left(\frac{\partial\lambda}{\partial n},\delta q\right)_{\Gamma_c} = 0\,,\\
&-(\nabla u,\nabla(\delta\lambda))_{\Omega} = 0\,,\\
&u = q \text{ on } \Gamma_c, \quad u = 0 \text{ on } \partial\Omega\setminus\Gamma_c, \quad \lambda = 0 \text{ on } \partial\Omega\,.
\end{aligned}$$

As noted above, this system implies the numerical implementation of the fractional Laplacian operator. Therefore, in the next section we introduce a numerical approximation of it.

$H^{1/2}(\Gamma_c)$ control. The only difference with respect to the previous case is the presence of the fractional norm in the objective functional and hence in the corresponding Lagrange functional.

The resulting optimality system is given by

$$\begin{aligned}
&((u-u_d),\delta u)_{\Omega_d} - (\nabla\lambda,\nabla(\delta u))_{\Omega} + \left(\frac{\partial\lambda}{\partial n},\delta u\right)_{\Gamma_c} = 0\,,\\
&\alpha(-\Delta_{\Gamma_c}^{\frac{1}{2}} q,\delta q)_{\Gamma_c} - \left(\frac{\partial\lambda}{\partial n},\delta q\right)_{\Gamma_c} = 0\,,\\
&-(\nabla u,\nabla(\delta\lambda))_{\Omega} = 0\,,\\
&u = q \text{ on } \Gamma_c, \quad u = 0 \text{ on } \partial\Omega\setminus\Gamma_c, \quad \lambda = 0 \text{ on } \partial\Omega\,.
\end{aligned}$$

$H^1(\Omega_c)$ control (lifting). The first-order necessary conditions for the lifting problem can be derived from the Lagrange functional

$$\mathcal{L}(\hat{u},\tilde{q},\lambda) = \frac{1}{2}\int_{\Omega_d} |\hat{u}+\tilde{q}-u_d|^2\,d\Omega + \frac{\alpha}{2}\left(\int_{\Omega_c} \tilde{q}^2\,dS + \int_{\Omega_c} |\nabla\tilde{q}|^2\,dS\right) - \int_{\Omega} \lambda(-\Delta(\hat{u}+\tilde{q}))\,d\Omega\,.$$

The optimality system reads, for all variations $\delta\hat{u} \in H^1(\Omega;\partial\Omega)$, $\delta\tilde{q} \in H^1(\Omega;\partial\Omega \setminus \Gamma_c)$ and $\delta\lambda \in H^1(\Omega;\partial\Omega)$,

$$
\begin{aligned}
&((\hat{u}+\tilde{q}-u_d),\delta\hat{u})_{\Omega_d} - (\nabla\lambda,\nabla(\delta\hat{u}))_\Omega = 0\,,\\
&((\hat{u}+\tilde{q}-u_d),\delta\tilde{q})_{\Omega_d} + \alpha[(\tilde{q},\delta\tilde{q})_{\Omega_c} + (\nabla\tilde{q},\nabla(\delta\tilde{q}))_{\Omega_c}] - (\nabla\lambda,\nabla(\delta\tilde{q}))_\Omega = 0\,,\\
&-(\nabla(\hat{u}+\tilde{q}),\nabla(\delta\lambda))_\Omega = 0\,,\\
&\hat{u} = 0 \text{ on } \partial\Omega, \quad \tilde{q} = 0 \text{ on } \partial\Omega \setminus \Gamma_c, \quad \lambda = 0 \text{ on } \partial\Omega\,.
\end{aligned}
$$

4. The Riesz fractional Laplacian and its numerical approximation

In this work, the numerical approximation of the fractional Laplacian operator on bounded domains is obtained through the Riesz fractional Laplacian. In order to correctly define it, we first introduce some basic definitions of the fractional Sobolev spaces.

Definition 2. *Given the open set in $\Omega \in \mathbb{R}^n$, the fractional Sobolev space $W^{s,p}(\Omega)$ is defined as*

$$
W^{s,p}(\Omega) = \left\{ u \in L^p(\Omega) : \frac{|u(\boldsymbol{x}) - u(\boldsymbol{y})|}{|\boldsymbol{x}-\boldsymbol{y}|^{\frac{n}{p}+s}} \in L^2(\Omega\times\Omega) \right\}, \tag{8}
$$

for any $p \in [1,+\infty)$ and with a fractional exponent $s \in (0,1)$.

Definition 3. *The natural norm in $W^{s,p}(\Omega)$ is defined as*

$$
\|u\|_{W^{s,p}(\Omega)} = \left(\int_\Omega |u|^p dx + \int_\Omega\int_\Omega \frac{|u(\boldsymbol{x}) - u(\boldsymbol{y})|^p}{|\boldsymbol{x}-\boldsymbol{y}|^{n+sp}} d\boldsymbol{x}\, d\boldsymbol{y} \right)^{\frac{1}{p}}.
$$

We also define the so-called Gagliardo semi-norm as

$$
[u]_{W^{s,p}(\Omega)} = \left(\int_\Omega\int_\Omega \frac{|u(\boldsymbol{x}) - u(\boldsymbol{y})|^p}{|\boldsymbol{x}-\boldsymbol{y}|^{n+sp}} d\boldsymbol{x}\, d\boldsymbol{y} \right)^{\frac{1}{p}}.
$$

In this work we will only consider the case $p = 2$, so that $W^{s,p}(\Omega) = H^s(\Omega)$ is a Hilbert space. In such case it holds

$$
W^{1,p}(\Omega) = H^1(\Omega) \subset H^s(\Omega)\,.
$$

From (8) we define the function space $H^s(\Omega)$ as

$$
H^s(\Omega) = \left\{ u \in L^2(\Omega) : \frac{|u(\boldsymbol{x}) - u(\boldsymbol{y})|}{|\boldsymbol{x}-\boldsymbol{y}|^{\frac{n}{2}+s}} \in L^2(\Omega\times\Omega) \right\}.
$$

For more information on fractional Sobolev spaces and norms, the interested reader can see [10].

We can now define the fractional Laplacian operator. First, we consider the generic Schwartz space $\mathcal{S}$ of rapidly decaying C^∞ functions in $\mathbb{R}^n$. Then, for any $u \in \mathcal{S}$ and $s \in (0,1)$, the fractional Laplacian $(-\Delta)^s$ is defined as

$$
(-\Delta)^s u(\boldsymbol{x}) = c_{n,s}\ P.V. \int_{\mathbb{R}^n} \frac{u(\boldsymbol{x}) - u(\boldsymbol{y})}{|\boldsymbol{x}-\boldsymbol{y}|^{n+2s}} d\boldsymbol{y}, \qquad 0 < s < 1\,, \tag{9}
$$

where *P.V.* means "in the principal value sense". $c_{n,s}$ depends only on s and on the dimensionality of the problem n. Its value can be written as

$$
c_{n,s} = C(n,s) = s\ 2^{2s}\ \frac{\Gamma(\frac{n+2s}{2})}{\pi^{n/2}\ \Gamma(1-s)}\,,
$$

where $\Gamma(k) = \int_0^\infty t^{k-1}e^{-t}dt$ is the well-known Gamma function. As introduced above, the Riesz fractional Laplacian is based on a direct implementation of the real space formula (9).

Note that the fractional operator can be seen as a special case of a nonlocal diffusion operator $\mathfrak{L}$ applied on the function $u(\boldsymbol{x}) : \Omega \to \mathbb{R}$ as

$$\mathfrak{L}u(\boldsymbol{x}) = 2\int_{\mathbb{R}^n} (u(\boldsymbol{y}) - u(\boldsymbol{x}))\gamma(\boldsymbol{x},\boldsymbol{y})d\boldsymbol{y}\ , \qquad \forall \boldsymbol{x} \in \Omega \subseteq \mathbb{R}^n\ , \tag{10}$$

where the kernel $\gamma(\boldsymbol{x},\boldsymbol{y}) : \Omega \times \Omega \to \mathbb{R}$ is a non-negative, symmetric mapping [8], defined as

$$\gamma(\boldsymbol{x},\boldsymbol{y}) = \frac{c_{n,s}}{2|\boldsymbol{x}-\boldsymbol{y}|^{n+2s}} \quad \forall \boldsymbol{x},\boldsymbol{y} \in \mathbb{R}^n\,.$$

4.1. Weak formulation. To illustrate the numerical implementation of the Riesz fractional Laplacian, we consider the simple steady-state nonlocal diffusion problem

$$\begin{cases} (-\Delta)^s u(\boldsymbol{x}) = f(\boldsymbol{x}) & \text{on } \Omega\,, \\ u(\boldsymbol{x}) = 0 & \text{on } \Gamma\,, \end{cases}$$

where Γ is the boundary of the domain Ω. Thus, the weak formulation of the considered problem reads as follows. Given the following spaces,

$$\begin{aligned} V &= \{v \in L^2(\Omega \cup \Gamma) : |||v||| < \infty \text{ and } v|_{\mathbb{R}^n \setminus \Omega} = 0\}\,, \\ V_0 &= \{v \in V : v|_\Gamma = 0\}, \end{aligned}$$

for $f \in V'$, find $u \in V$ such that

$$\mathcal{A}(u,v) = \mathcal{F}(v)\,, \qquad \forall v \in V_0\,, \qquad \text{subject to } u = 0 \text{ on } \Gamma\,, \tag{11}$$

where

$$\begin{aligned} \mathcal{A}(u,v) &= \frac{c_{n,s}}{2}\int_{\mathbb{R}^n}\int_{\mathbb{R}^n} \frac{u(\boldsymbol{y})-u(\boldsymbol{x})}{|\boldsymbol{x}-\boldsymbol{y}|^{n+2s}}\big(v(\boldsymbol{y})-v(\boldsymbol{x})\big)\ d\boldsymbol{y}\ d\boldsymbol{x}\,, \\ \mathcal{F}(v) &= \int_\Omega f v\ d\boldsymbol{x}\ . \end{aligned} \tag{12}$$

Here, the *energy* semi-norm $|||\cdot|||$ is defined as

$$|||v|||^2 = \mathcal{A}(v,v),$$

and the space V' is the dual space of V.

The restriction of (12) on the domain Ω is obtained by imposing

$$u(\boldsymbol{x}) = 0,\ v(\boldsymbol{x}) = 0 \quad \forall \boldsymbol{x} \in \mathbb{R}^n \setminus \Omega\ . \tag{13}$$

In this work we use a semi-analytical technique instead of the interaction radius method. In particular, to simplify the notation we introduce

$$\mathcal{X}(\boldsymbol{x},\boldsymbol{y}) = \frac{c_{n,s}}{2}\frac{u(\boldsymbol{y})-u(\boldsymbol{x})}{|\boldsymbol{x}-\boldsymbol{y}|^{n+2s}}\big(v(\boldsymbol{y})-v(\boldsymbol{x})\big)\,.$$

We now split the double integral in (12) as

$$\begin{aligned} \mathcal{A}(u,v) = &\int_\Omega\int_\Omega \mathcal{X}(\boldsymbol{x},\boldsymbol{y})\ d\boldsymbol{y}d\boldsymbol{x} + \int_{\mathbb{R}^n\setminus\Omega}\int_\Omega \mathcal{X}(\boldsymbol{x},\boldsymbol{y})\ d\boldsymbol{y}d\boldsymbol{x} \\ &+ \int_\Omega\int_{\mathbb{R}^n\setminus\Omega} \mathcal{X}(\boldsymbol{x},\boldsymbol{y})\ d\boldsymbol{y}d\boldsymbol{x} + \int_{\mathbb{R}^n\setminus\Omega}\int_{\mathbb{R}^n\setminus\Omega} \mathcal{X}(\boldsymbol{x},\boldsymbol{y})\ d\boldsymbol{y}d\boldsymbol{x}\,. \end{aligned}$$

Now, by applying the restriction (13) we have

$$\int_{\mathbb{R}^n \setminus \Omega} \int_{\mathbb{R}^n \setminus \Omega} \mathcal{X}(\boldsymbol{x}, \boldsymbol{y}) \, d\boldsymbol{y} d\boldsymbol{x} = 0 \,.$$

Therefore, the numerical implementation of the fractional Laplacian can be split into a bounded contribution $\mathcal{B}(u,v) = \int_\Omega \int_\Omega \mathcal{X}(\boldsymbol{x}, \boldsymbol{y}) \, d\boldsymbol{y} d\boldsymbol{x}$, and an unbounded contribution, represented by the two integrals $\mathcal{C}(u,v) = \int_{\mathbb{R}^n \setminus \Omega} \int_\Omega \mathcal{X}(\boldsymbol{x}, \boldsymbol{y}) \, d\boldsymbol{y} d\boldsymbol{x}$ and $\int_\Omega \int_{\mathbb{R}^n \setminus \Omega} \mathcal{X}(\boldsymbol{x}, \boldsymbol{y}) \, d\boldsymbol{y} d\boldsymbol{x}$. Moreover, since $\mathcal{X}(\boldsymbol{x}, \boldsymbol{y}) = \mathcal{X}(\boldsymbol{y}, \boldsymbol{x})$, it holds

$$\mathcal{A}(u,v) = \mathcal{B}(u,v) + \mathcal{C}(u,v) = \int_\Omega \int_\Omega \mathcal{X}(\boldsymbol{x}, \boldsymbol{y}) d\boldsymbol{y} d\boldsymbol{x} + 2 \int_\Omega \int_{\mathbb{R}^n \setminus \Omega} \mathcal{X}(\boldsymbol{x}, \boldsymbol{y}) d\boldsymbol{y} d\boldsymbol{x} \,, \tag{14}$$

subject to (13). We now introduce a simple semi-analytical model to approximate the integral over $\mathbb{R}^n \setminus \Omega$ in the unbounded term.

4.2. A semi-analytical approach to the unbounded integral. We now consider the unbounded term under the condition (13), obtaining

$$\mathcal{C}(u,v) = c_{n,s} \int_\Omega u(\boldsymbol{x}) v(\boldsymbol{x}) \int_{\mathbb{R}^n \setminus \Omega} \frac{1}{|\boldsymbol{x} - \boldsymbol{y}|^{n+2s}} \, d\boldsymbol{y} \, d\boldsymbol{x} \,.$$

We describe how to perform the integration on one- and two-dimensional domains, since in this work we are interested in handling the fractional Laplacian on boundaries of two- and three-dimensional domains.

If we consider a one-dimensional domain, the inner integral can be evaluated analytically. In fact, if we consider $\Omega = [a,b]$, $a, b \in \mathbb{R}$, $a > b$, we have $\forall x \in]a,b[$

$$\begin{aligned}
\int_{\mathbb{R}^n \setminus \Omega} \frac{1}{|x-y|^{n+2s}} \, dy &= \int_{-\infty}^{a} \frac{1}{|x-y|^{n+2s}} \, dy + \int_{b}^{\infty} \frac{1}{|x-y|^{n+2s}} \, dy \\
&= \frac{1}{n+2s-1} \left(\left[\frac{1}{|x-y|^{n+2s-1}} \right]_{-\infty}^{a} + \left[\frac{1}{|x-y|^{n+2s-1}} \right]_{b}^{\infty} \right) \\
&= \frac{1}{n+2s-1} \left(\frac{1}{(x-a)^{n+2s-1}} + \frac{1}{(b-x)^{n+2s-1}} \right) .
\end{aligned}$$

For a two-dimensional case, the integral over $\mathbb{R}^n \setminus \Omega$ cannot be analytically evaluated. Thus, we introduce now a semi-analytical technique to approximate the unbounded integral.

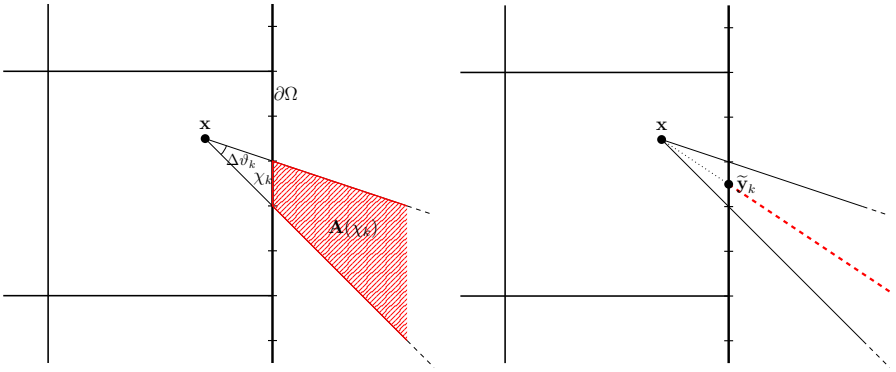

FIGURE 1. Area of numerical integration (left) and integration line (right) for one of the subdivisions of $\partial\Omega$.

Similarly to the technique presented in [17], a technique based on a mapping of the unbounded integral over the boundary $\partial\Omega$ is presented. In particular, we split each boundary element into n_{sub} subdivisions. Then, the whole boundary is divided into N_{sub} subdivisions χ_k, $k \in [1, N_{sub}]$. Each subdivision intercepts an area $A(\chi_k)$, such that $\bigcup_k A(\chi_k) = \{\mathbb{R}^n \setminus \Omega\}$, as reported in Figure 1 on the left. So we obtain

$$\int_{\mathbb{R}^n \setminus \Omega} \frac{1}{|\boldsymbol{x}-\boldsymbol{y}|^{n+2s}}\, d\boldsymbol{y} = \sum_{k=1}^{N_{sub}} \int_{A(\chi_k)} \frac{1}{|\boldsymbol{x}-\boldsymbol{y}|^{n+2s}}\, d\boldsymbol{y}\ .$$

The integrals over $A(\chi_k)$ are approximated along the line connecting $\boldsymbol{x}$ and $\widetilde{\boldsymbol{y}}_k$, that is the midpoint of the segment χ_k. Therefore, considering $d = |\boldsymbol{x} - \widetilde{\boldsymbol{y}}_k|$ the approximate integral becomes

$$\begin{aligned}\int_{A(\chi_k)} \frac{1}{|\boldsymbol{x}-\boldsymbol{y}|^{n+2s}}\, d\boldsymbol{y} \ &\simeq \Delta\vartheta_k \int_d^{+\infty} \frac{1}{t^{n+2s}} dt = \frac{\Delta\vartheta_k}{1-n-2s}\left[\frac{1}{t^{n+2s-1}}\right]_d^{+\infty} \\ &= \frac{\Delta\vartheta_k}{(n+2s-1)|\boldsymbol{x}-\widetilde{\boldsymbol{y}}_k|^{n+2s-1}}\,.\end{aligned}$$

4.3. The fractional Laplacian FEM formulation. To introduce the FE discretization of the presented problem, let $\mathcal{T}_h$ be a shape-regular triangulation of Ω into N_L finite elements $\{\mathcal{E}_l\}_{l=1}^{N_L}$. The finite elements can either be triangles or quadrilaterals in two dimensions and tetrahedra or hexaheadra in three dimensions. The parameter h represents the size of the triangulation and corresponds to the larger element diameter. Also, let $V_0^{N_h}$ be a finite dimensional subspace of V_0 of dimension N_h, proportional to h^{-1}, and let $\{v_i\}_{i=1}^{N_h}$ be a basis for $V_0^{N_h}$. In this work we consider Lagrange basis functions over the triangulation $\mathcal{T}_h$. Thus, we can write the FE solution u_h of equation (11) as $u_h(\boldsymbol{x}) = \sum_{i=1}^{N_h} U_i v_i(\boldsymbol{x})$. By using this expression and $v \in \{v_i\}_{i=1}^{N_h}$, and considering the split (14), the equation (11) reduces to the algebraic system

$$A\boldsymbol{U} = (B + C)\boldsymbol{U} = \boldsymbol{F},$$

where $\boldsymbol{U} \in \mathbb{R}^{N_h}$ is the vector whose components are the degrees of freedom of the numerical solution u_h, B is the stiffness matrix with entries

$$B_{ij} = \int_\Omega \int_\Omega \left(\varphi_i(\boldsymbol{x}) - \varphi_i(\boldsymbol{y})\right)\left(\varphi_j(\boldsymbol{x}) - \varphi_j(\boldsymbol{y})\right)\gamma(\boldsymbol{x},\boldsymbol{y}) d\boldsymbol{y}\, d\boldsymbol{x}\,, \tag{15}$$

and C is the stiffness matrix with entries

$$C_{ij} = c_{n,s} \int_\Omega \varphi_i(\boldsymbol{x})\varphi_j(\boldsymbol{x}) \sum_{k=1}^{N_{sub}} \frac{\Delta\vartheta_k}{(n+2s-1)|\boldsymbol{x}-\widetilde{\boldsymbol{y}}_k|^{n+2s-1}} d\boldsymbol{x}\,.$$

For implementation purposes, it is convenient to rewrite the matrix (15) as $B_{ij} = B_{ij}^{11} + B_{ij}^{12} + B_{ij}^{21} + B_{ij}^{22}$, where

$$B_{ij}^{11} = \int_\Omega \int_\Omega \varphi_i(\boldsymbol{x})\varphi_j(\boldsymbol{x})\gamma(\boldsymbol{x},\boldsymbol{y})d\boldsymbol{y}\, d\boldsymbol{x}\,,$$
$$B_{ij}^{12} = -\int_\Omega \int_\Omega \varphi_i(\boldsymbol{x})\varphi_j(\boldsymbol{y})\gamma(\boldsymbol{x},\boldsymbol{y})d\boldsymbol{y}\, d\boldsymbol{x}\,,$$
$$B_{ij}^{21} = -\int_\Omega \int_\Omega \varphi_i(\boldsymbol{y})\varphi_j(\boldsymbol{x})\gamma(\boldsymbol{x},\boldsymbol{y})d\boldsymbol{y}\, d\boldsymbol{x}\,,$$
$$B_{ij}^{22} = \int_\Omega \int_\Omega \varphi_i(\boldsymbol{y})\varphi_j(\boldsymbol{y})\gamma(\boldsymbol{x},\boldsymbol{y})d\boldsymbol{y}\, d\boldsymbol{x}\,.$$

As noted in [21], since the kernel $\gamma(\boldsymbol{x},\boldsymbol{y})$ is symmetrical, we can simplify the numerical implementation of B_{ij} considering $B_{ij} = 2B_{ij}^{11} + 2B_{ij}^{12} = 2B_{ij}^{21} + 2B_{ij}^{22}$.

Note that the resulting B_{ij} matrix is a dense matrix. This implies higher computational cost in the numerical resolution of an optimal boundary control problem with fractional regularization. However, the portion of the domain where the fractional operator is calculated is a boundary by construction, so the increase of computational cost is limited (e.g. for $n = 3$ the fractional operator shall be calculated on a two-dimensional boundary, with a mild effect on the overall sparsity pattern of the matrix).

5. The addition of control inequality constraints

All the proposed boundary optimal control formulations can be considered in conjunction with inequality constraints on the control variable:

$$q_{min} \leq q \leq q_{max} \text{ a.e. on } \Gamma_c\,,$$

where $q_{min}, q_{max} \in L^\infty(\Gamma_c)$.

Constraints of inequality type play an important role, in particular when the control variable - which is the input that can steer the behavior of the system - must be bound between certain maximum and minimum values for practical considerations.

In the following, we briefly describe how control inequality constraints were enforced in this work. For simplicity, we do so for the discretization of the optimality system arising from the $H^{1/2}(\Gamma_c)$ approach, thus from Problem 1 under the condition (7). Similar descriptions hold for the other optimality systems.

The discrete optimality systems arising from all the presented regularization methods can be cast as algebraic systems that exhibit a block structure. First we present the block structure without inequality constraints. We have

$$\begin{bmatrix} M_{\Omega_d} & 0 & -\Delta_\Omega + \left.\dfrac{\partial}{\partial n}\right|_{\Gamma_c} \\ 0 & \alpha F_{\Gamma_c} & -\left.\dfrac{\partial}{\partial n}\right|_{\Gamma_c} \\ -\Delta_\Omega & 0 & 0 \end{bmatrix} \begin{bmatrix} u_h \\ q_h \\ \lambda_h \end{bmatrix} = \begin{bmatrix} M_{\Omega_d} u_d \\ 0 \\ 0 \end{bmatrix},$$

where u_h, q_h and λ_h denote the discretized state, control and adjoint variables, respectively. The blocks $M_{\mathcal{O}}$, $-\Delta_{\mathcal{O}}$ and $\left.\dfrac{\partial}{\partial n}\right|_{\mathcal{O}}$ denote the mass matrix, the Laplacian matrix and boundary Neumann matrix with integration over the generic domain $\mathcal{O}$, respectively. Moreover, $F_{\mathcal{O}}$ represents the matrix corresponding to the numerical implementation of the fractional Laplacian on $\mathcal{O}$.

The enforcement of the inequality constraints can be achieved using the *Primal-Dual Active Set* (PDAS) method, which was first proposed in [25]. Each iteration of the method consists in the solution of a linear system

$$\mathcal{M}_k \delta \boldsymbol{u}_{k+1} = f(\boldsymbol{u}_k)\,,$$

where $\mathcal{M}_k$ can be written as a 4×4 block structure. The upper-left 3×3 block is the same as before, while one block row and one block column are added, together with the variable μ:

$$\mathcal{M}_k = \begin{bmatrix} M_{\Omega_d} & 0 & -\Delta_\Omega + \left.\dfrac{\partial}{\partial n}\right|_{\Gamma_c} & 0 \\ 0 & \alpha F_{\Gamma_c} & -\left.\dfrac{\partial}{\partial n}\right|_{\Gamma_c} & I_{\Gamma_c} \\ -\Delta_\Omega & 0 & 0 & 0 \\ 0 & c\Pi_{\mathcal{A}_k} & 0 & \Pi_{I_k} \end{bmatrix}.$$

The terms $\delta \boldsymbol{u}_{k+1}$ and $f(\boldsymbol{u}_k)$ read

$$\delta \boldsymbol{u}_{k+1} = \begin{bmatrix} \delta u_{k+1} \\ \delta q_{k+1} \\ \delta \lambda_{k+1} \\ \delta \mu_{k+1} \end{bmatrix} = \begin{bmatrix} u_{k+1} - u_k \\ q_{k+1} - q_k \\ \lambda_{k+1} - \lambda_k \\ \mu_{k+1} - \mu_k \end{bmatrix},$$

$$f(\boldsymbol{u}_k) = -\begin{bmatrix} M_{\Omega_d}(u_k - u_d) - \Delta_\Omega \lambda_k + \left.\dfrac{\partial \lambda_k}{\partial n}\right|_{\Gamma_c} \\ \alpha F_{\Gamma_c} q_k - \left.\dfrac{\partial \lambda_k}{\partial n}\right|_{\Gamma_c} + I_{\Gamma_c} \mu_k \\ -\Delta_\Omega u_k \\ c\Pi_{\mathcal{A}_k} q_k + \Pi_{I_k} \mu_k - c(\Pi_{\mathcal{A}_k^b} q_{max} + \Pi_{\mathcal{A}_k^a} q_{min}) \end{bmatrix}.$$

For a complete definition of all the additional blocks, such as $\Pi_{\mathcal{A}_k}$, Π_{I_k} and I_{Γ_c}, the interested reader can consult [24].

6. Numerical results

In this section, we compare the numerical solution of the optimality systems associated to the various formulations of boundary optimal control problems presented above. We consider both two-dimensional and three-dimensional domains, as well as the absence or presence of inequality constraints.

6.1. Cases without inequality constraint. We first aim to solve the optimal control problems presented in section 2 without inequality constraints. We consider both a two-dimensional and a three-dimensional domain, as reported in Figure 6.1. In particular, in the two-dimensional case we consider a domain $\Omega = \{x \in [0,1],\, y \in [0,1]\}$, a control domain $\Gamma_c = \{x \in [0.25, 0.75],\, y = 0\}$, and a target domain $\Omega_d = \{x \in [0,1],\, y \in [0, 0.5]\}$. For the lifting control approach, we choose a domain for the lifting function $\Omega_c = \{x \in [0.25, 0.75],\, y \in [0,1]\}$.

In the three-dimensional case, we consider a domain $\Omega = \{x \in [0,1],\, y \in [0,1],\, z \in [0,1]\}$, a control surface $\Gamma_c = \{x \in [0.25, 0.75],\, y \in [0,1],\, z = 0\}$, and $\Omega_d = \{x \in [0,1],\, y \in [0.5,1],\, z \in [0,1]\}$. For the lifting control, we choose $\Omega_c = \{x \in [0.25, 0.75],\, y \in [0,1],\, z \in [0,1]\}$.

At the coarse level, the 2D domain is discretized with a 2×2 uniform grid of quadrilaterals, while the 3D domain is discretized with a $4 \times 2 \times 1$ uniform grid

of hexahedra. In the following, results will be reported for various refinements of these coarse meshes. All variables of the optimality systems are discretized with piecewise-continuous biquadratic (in 2D) or triquadratic (in 3D) Lagrange finite element families. All the numerical tests were obtain using a GMRES solver with ILU preconditioner.

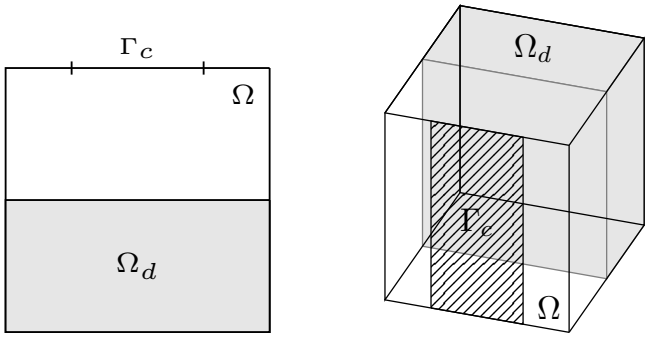

FIGURE 2. Two-dimensional (left) and three-dimensional (right) domain used for the presented numerical simulations. The domain of Γ_c and Ω_d are highlighted.

Two-dimensional case. We first consider the two-dimensional control problems, and we compare the numerical results of all the regularization techniques introduced above. In particular, we consider $u_d = 1$, and we evaluate the effectiveness of the implemented control algorithm through the distance from the objective $0.5 \int_{\Omega_d} (u - u_d)^2 d\boldsymbol{x}$.

TABLE 1. Two-dimensional case: distance from the objective for different mesh refinements N_{lev} and regularization parameter α for fractional regularization ($s = 0.5$), H^1 regularization ($s = 1$), and lifting function approach (lift.).

$0.5 \int_{\Omega_d} (u - u_d)^2 d\boldsymbol{x}$

	$N_{lev} = 4$			$N_{lev} = 5$		
α	$s = 0.5$	$s = 1$	lift.	$s = 0.5$	$s = 1$	lift.
10^{-1}	0.247733	0.249751	0.248430	0.247708	0.249751	0.248401
10^{-2}	0.229612	0.247544	0.235424	0.229410	0.247539	0.235178
10^{-3}	0.152829	0.228103	0.167513	0.152410	0.228059	0.166781
10^{-4}	0.112894	0.149903	0.114396	0.112854	0.149821	0.114340
10^{-5}	0.111212	0.112843	0.111306	0.111196	0.112838	0.111321
10^{-6}	0.110343	0.111431	0.110784	0.110286	0.111430	0.110577
10^{-7}	0.105704	0.111024	0.107450	0.105543	0.111013	0.106354

In Table 1 we report the distance from the objective for the fractional regularization, the H^1 regularization and the lifting function approach. We investigated different values of the regularization parameter α and different mesh refinements.

For all the tested cases, the distance from the objective decreases as the value of α decreases, consistently with the expectations. In fact, lower values of the regularization parameter imply that the tracking term is predominant in the functional $\mathcal{J}$ in (3). Moreover, the results obtained with the fractional regularization show a slightly lower distance from the objective in comparison with the H^1 regularization, as expected from the theoretical results: in fact, as noted above, the H^1 regularization imposes the solution in a more restrictive function space than the natural one. The results obtained with the lifting function approach show a behavior similar to the fractional results, as expected. Moreover, the refinement of the mesh does not affect significantly the numerical solution of the algorithm.

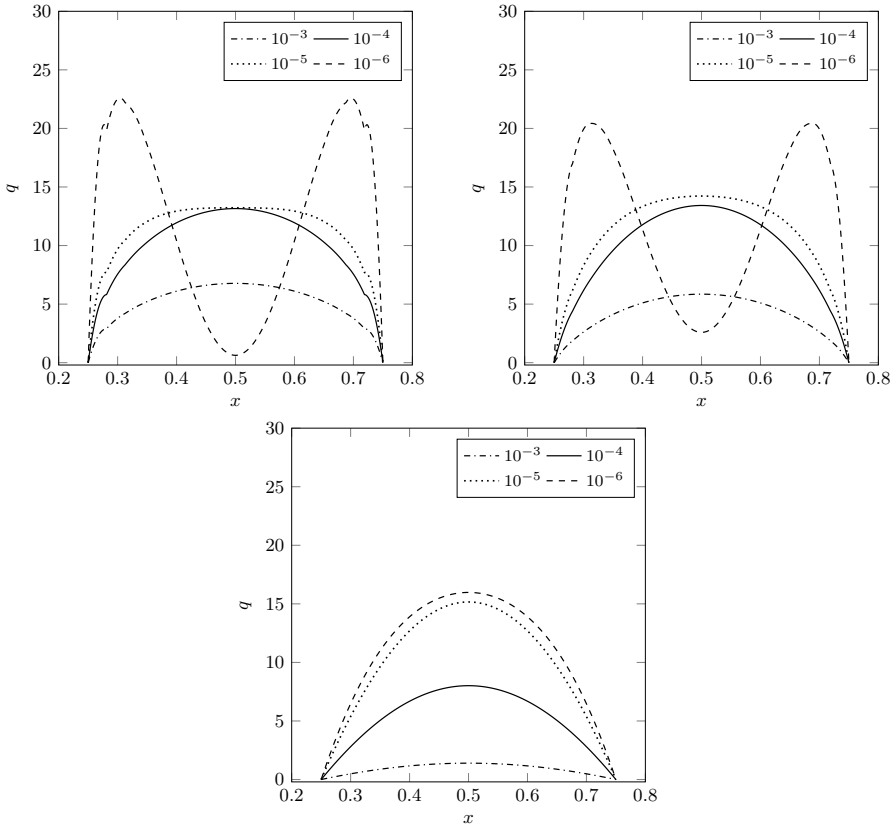

FIGURE 3. Two-dimensional test case: control variable on Γ_c with $N_{lev} = 5$ for $\alpha = 10^{-3}$, 10^{-4}, 10^{-5} and 10^{-6}, with fractional (top left), lifting (top right) and H^1 (bottom) regularization.

In Figure 3 we report the control q fields on Γ_c for the two-dimensional case with $N_{lev} = 5$ for various α values, for both fractional, H^1 regularization and lifting function approach. Note that the used regularization parameter strongly affects the control field. The general trend of the fractional and the lifting controls is qualitatively similar. This can be taken as an indication that the two methods are in good agreement and they search for optimal boundary controls in the same trace space.

Three-dimensional case. We now consider the three-dimensional case of the optimal control problems, to extend the investigation carried out for two-dimensional domains. The numerical domain was depicted in Figure 6.1.

TABLE 2. Three-dimensional case: distance from the objective for different mesh refinements N_{lev} and regularization parameter α for fractional regularization ($s = 0.5$), H^1 regularization ($s = 1$), and lifting function approach (lifting).

$0.5 \int_{\Omega_d} (u - u_d)^2 d\boldsymbol{x}$

	$N_{lev} = 2$			$N_{lev} = 3$		
α	$s = 0.5$	$s = 1$	lift.	$s = 0.5$	$s = 1$	lift.
10^{-1}	0.249689	0.249968	0.248904	0.249666	0.249966	0.248533
10^{-2}	0.246949	0.249685	0.239601	0.246732	0.249657	0.236313
10^{-3}	0.224625	0.246913	0.182321	0.223201	0.246644	0.170258
10^{-4}	0.162464	0.224386	0.116851	0.161762	0.222628	0.114594
10^{-5}	0.146361	0.162361	0.111321	0.146895	0.161462	0.111162
10^{-6}	0.146019	0.146602	0.111238	0.144712	0.147245	0.111045
10^{-7}	0.146903	0.146319	0.111237	0.137633	0.145645	0.110388

In Table 2 we report the distance from the objective for all the tested cases. Similarly to the two-dimensional case, we report the results depending on the regularization parameter α and on the refinement level N_{lev}. Differently from the two-dimensional case, the lifting function approach shows numerical results closer to the objective in comparison with the numerical results obtained using both the fractional and the H^1 regularization. Thus, the lifting function proves to be the best performing regularization technique in terms of distance from the objective. The numerical results obtained with the finer mesh are closer to the objective with a coarser mesh.

Comparison of assembly and solver times. In Tables 3 and 4 we report some results to assess the performance of the proposed methods in terms of computational time for a two- or three-dimensional case, respectively. Here, the two-dimensional mesh was generated from 5 mesh refinements of the coarse grid, while the three-dimensional one was obtained with 3 refinements.

First of all, we notice for all cases that both assembly time (the time to build the linear system resulting from the finite element discretization of the optimality system) and solver time (the time to perform the numerical solution) are basically independent of α.

We also observe that assembly times are shorter for $H^1(\Gamma_c)$ boundary controls, then slightly longer for the lifting approach and they are significantly longer for the $H^{1/2}(\Gamma_c)$ formulation. This is clearly attributed to the presence of the double integral in the fractional Laplacian. Concerning solver times, they appear to be comparable for the lifting case as well as for the $H^1(\Gamma_c)$ case, while they are longer for the $H^{1/2}(\Gamma_c)$ case. These results suggest that the lifting approach is a viable alternative to a pure fractional formulation, as it yields similar results in terms of optimization with smaller computational times.

TABLE 3. Two-dimensional case: assembly times and solver times (in seconds) for different regularization parameters α for fractional regularization ($s = 0.5$), H^1 regularization ($s = 1$), and lifting function approach (lift.)

	Assembly time			Solver time		
α	$s = 0.5$	$s = 1$	lift.	$s = 0.5$	$s = 1$	lift.
10^{-1}	0.55721	0.116872	0.134791	0.885629	0.565865	0.514959
10^{-2}	0.565082	0.119016	0.13571	0.911642	0.56159	0.513302
10^{-3}	0.547106	0.117627	0.136169	0.879698	0.568431	0.513778
10^{-4}	0.544492	0.117966	0.135277	0.875263	0.574497	0.511519
10^{-5}	0.550626	0.116844	0.140617	0.889002	0.564336	0.522148
10^{-6}	0.550696	0.116792	0.135128	0.877142	0.565352	0.520729
10^{-7}	0.572248	0.117626	0.136023	0.910968	0.571587	0.522958

TABLE 4. Three-dimensional case: assembly times and solver times (in seconds) for different regularization parameters α for fractional regularization ($s = 0.5$), H^1 regularization ($s = 1$), and lifting function approach (lift.)

	Assembly time			Solver time		
α	$s = 0.5$	$s = 1$	lift.	$s = 0.5$	$s = 1$	lift.
10^{-1}	5.653254	1.003316	1.752929	4.258652	2.641471	2.673116
10^{-2}	5.643262	1.001714	1.757769	4.266891	2.666312	2.700669
10^{-3}	5.654477	1.003768	1.754325	4.258153	2.640889	2.703094
10^{-4}	5.664297	1.002984	1.748731	4.266532	2.642459	2.807016
10^{-5}	5.660745	1.022653	1.756247	4.260642	2.711065	2.819473
10^{-6}	5.655265	1.055839	1.750449	4.261726	2.728984	2.85426
10^{-7}	5.648923	1.004636	1.771234	5.344629	2.738823	2.906721

6.2. Cases with inequality constraint. We now show that the presence of control inequality constraints yields solutions that are more distant from the desired target. Also, the inequality bound limits the norms of the control, for all proposed formulations. We solve the numerical system introduced in section 5, and we consider two different maximum values of the control variable q.

In particular, in Table 5 we report the numerical results considering $q_{max} = 5$. As can be noted from Figure 3, the results are basically locked by the imposed limit, depending on the value of α. Since a decrease in α implies an increase of the norm of q calculated on Γ_c, the distance from the objective for low α values is the same in all these cases. In the Table we also report in parentheses the number of iterations needed by the algorithm to find the solution with the inequality constraint. As a general behavior, it can be noted that the H^1 regularization needs fewer iterations to find the solution, followed by the fractional regularization, and by the lifting function approach.

In Table 6, we report the results obtained with $q_{max} = 0.01$. The distance from the objective is the same in all the tested cases, meaning that the inequality bound

TABLE 5. Two-dimensional case: distance from the objective and iterations of the algorithm (shown in brackets) for different mesh refinements N_{lev} and regularization parameters α for fractional regularization ($s = 0.5$), H^1 regularization ($s = 1$), and lifting function approach (lift.) with an inequality constraint of $q_{max} = 5$.

$0.5 \int_{\Omega_d} (u - u_d)^2 d\boldsymbol{x}$

	$N_{lev} = 4$			$N_{lev} = 5$		
α	$s = 0.5$	$s = 1$	lift.	$s = 0.5$	$s = 1$	lift.
10^{-1}	0.24773(2)	0.24975(2)	0.24839(2)	0.24771(2)	0.24975(2)	0.24839(2)
10^{-2}	0.22961(2)	0.24754(2)	0.23520(2)	0.22941(2)	0.24754(2)	0.23509(2)
10^{-3}	0.16545(5)	0.22810(2)	0.17145(4)	0.16518(5)	0.22806(2)	0.17140(4)
10^{-4}	0.15881(3)	0.17235(5)	0.15881(6)	0.15765(4)	0.17236(7)	0.15793(5)
10^{-5}	0.15881(3)	0.16145(3)	0.15881(5)	0.15765(4)	0.16144(4)	0.15765(6)
10^{-6}	0.15881(4)	0.15881(4)	0.15881(6)	0.15765(4)	0.15765(4)	0.15765(6)
10^{-7}	0.15881(5)	0.15881(3)	0.15881(7)	0.15765(4)	0.15765(4)	0.15765(8)

TABLE 6. Two-dimensional case: distance from the objective and iterations of the algorithm (shown in brackets) for different mesh refinements N_{lev} and regularization parameters α for fractional regularization ($s = 0.5$), H^1 regularization ($s = 1$), and lifting function approach (lift.) with an inequality constraint of $q_{max} = 0.01$.

$0.5 \int_{\Omega_d} (u - u_d)^2 d\boldsymbol{x}$

	$N_{lev} = 4$			$N_{lev} = 5$		
α	$s = 0.5$	$s = 1$	lift.	$s = 0.5$	$s = 1$	lift.
10^{-1}	0.24977(3)	0.24982(6)	0.24977(5)	0.24977(3)	0.24982(9)	0.24977(5)
10^{-2}	0.24977(3)	0.24978(4)	0.24977(5)	0.24977(3)	0.24978(7)	0.24977(5)
10^{-3}	0.24977(3)	0.24977(3)	0.24977(5)	0.24977(3)	0.24977(4)	0.24977(5)
10^{-4}	0.24977(3)	0.24977(3)	0.24977(5)	0.24977(3)	0.24977(3)	0.24977(5)
10^{-5}	0.24977(3)	0.24977(3)	0.24977(5)	0.24977(3)	0.24977(3)	0.24977(5)
10^{-6}	0.24977(3)	0.24977(3)	0.24977(5)	0.24977(3)	0.24977(3)	0.24977(5)
10^{-7}	0.24977(4)	0.24977(3)	0.24977(7)	0.24977(4)	0.24977(3)	0.24977(7)

works properly. The tests show a different number of iterations, with the same trend as for the case with $q_{max} = 5$.

7. Conclusions

In this work we presented and compared several regularization methods for the treatment of boundary optimal control problems constrained by PDEs and with control inequality constraints. We proposed two formulations that avoid a mismatch between the boundary regularity of optimal states and that of boundary optimal controls. In particular, the first formulation is based on the direct presence of fractional Sobolev boundary control norms in the objective functional. The resulting optimality system is then characterized by the presence of a fractional Laplacian operator, whose numerical discretization has been dealt with by a semi-analytical method. The second formulation is based on the introduction of lifting functions. We investigated their numerical performance on two- and three-dimensional test cases. Both the lifting function and the fractional approach show a similar distance from the objective for two-dimensional simulations, while

the lifting function approach shows a smaller distance from the objective in three-dimensional tests. More importantly, the lifting function approach exhibits smaller assembly and solver times. These results lead to the observation that the lifting function approach is a valuable method for boundary optimal control computations. Additional numerical results show that all the proposed formulations can be easily integrated with control inequality constraints. Multiple directions of further investigation may stem from the model setup considered here. In particular, the comparison of the proposed methods to the case of other constraint equations is subject of current research.

References

[1] M. Gunzburger, L. Hou, and T. P. Svobodny, Analysis and finite element approximation of optimal control problems for the stationary Navier-Stokes equations with Dirichlet controls, ESAIM: Mathematical Modelling and Numerical Analysis, vol. 25, no. 6, pp. 711–748, 1991.

[2] M. D. Gunzburger, L. Hou, and T. P. Svobodny, Analysis and finite element approximation of optimal control problems for the stationary Navier-Stokes equations with distributed and Neumann controls, Mathematics of Computation, vol. 57, no. 195, pp. 123–151, 1991.

[3] A. Chierici, L. Chirco, and S. Manservisi, Optimal Pressure Boundary Control of Steady Multiscale Fluid-Structure Interaction Shell Model Derived from Koiter Equations, Fluids, vol. 6, no. 4, p. 149, 2021.

[4] G. Bornia, M. Gunzburger, and S. Manservisi, A distributed control approach for the boundary optimal control of the steady MHD equations, Communications In Computational Physics, vol. 14, no. 3, pp. 722–752, 2013.

[5] E. Aulisa, G. Bornia, and S. Manservisi, Boundary control problems in convective heat transfer with lifting function approach and multigrid Vanka-type solvers, Communications in Computational Physics, vol. 18, no. 3, pp. 621–649, 2015.

[6] G. Bornia and S. Ratnavale, Different approaches for Dirichlet and Neumann boundary optimal control, in AIP Conference Proceedings, vol. 1978, p. 270006, AIP Publishing LLC, 2018.

[7] L. Chirco, A. Chierici, R. Da Vià, V. Giovacchini, and S. Manservisi, Optimal Control of the Wilcox turbulence model with lifting functions for flow injection and boundary control, in Journal of Physics: Conference Series, vol. 1224, p. 012006, IOP Publishing, 2019.

[8] M. D'Elia and M. Gunzburger, The fractional Laplacian operator on bounded domains as a special case of the nonlocal diffusion operator, Computers & Mathematics with Applications, vol. 66, no. 7, pp. 1245–1260, 2013.

[9] M. D'Elia, Q. Du, C. Glusa, M. Gunzburger, X. Tian, and Z. Zhou, Numerical methods for nonlocal and fractional models, Acta Numerica, vol. 29, pp. 1–124, 2020.

[10] E. Di Nezza, G. Palatucci, and E. Valdinoci, Hitchhikers guide to the fractional Sobolev spaces, Bulletin des sciences mathématiques, vol. 136, no. 5, pp. 521–573, 2012.

[11] A. Bonito, J. P. Borthagaray, R. H. Nochetto, E. Otárola, and A. J. Salgado, Numerical methods for fractional diffusion, Computing and Visualization in Science, vol. 19, no. 5-6, pp. 19–46, 2018.

[12] R. Čiegis, V. Starikovičius, S. Margenov, and R. Kriauzienė, A comparison of accuracy and efficiency of parallel solvers for fractional power diffusion problems, in International Conference on Parallel Processing and Applied Mathematics, pp. 79–89, Springer, 2017.

[13] S. Duo, H. Wang, and Y. Zhang, A comparative study on nonlocal diffusion operators related to the fractional laplacian, Discrete and Continuous Dynamical Systems - Series B, vol. 24, no. 1, pp. 231–256, 2019.

[14] A. Bonito and J. Pasciak, Numerical approximation of fractional powers of elliptic operators, Mathematics of Computation, vol. 84, no. 295, pp. 2083–2110, 2015.

[15] A. Bonito and J. E. Pasciak, Numerical approximation of fractional powers of regularly accretive operators, IMA Journal of Numerical Analysis, vol. 37, no. 3, pp. 1245–1273, 2017.

[16] A. Bonito, W. Lei, and J. E. Pasciak, Numerical approximation of the integral fractional Laplacian, Numerische Mathematik, vol. 142, no. 2, pp. 235–278, 2019.

[17] A. Lischke, G. Pang, M. Gulian, F. Song, C. Glusa, X. Zheng, Z. Mao, W. Cai, M. M. Meerschaert, M. Ainsworth, et al., What is the fractional Laplacian? A comparative review with new results, Journal of Computational Physics, vol. 404, p. 109009, 2020.
[18] M. DElia, M. Gulian, H. Olson, and G. E. Karniadakis, Towards a unified theory of fractional and nonlocal vector calculus, Fractional Calculus and Applied Analysis, vol. 24, no. 5, pp. 1301–1355, 2021.
[19] C. Cortazar, M. Elgueta, J. D. Rossi, and N. Wolanski, How to approximate the heat equation with Neumann boundary conditions by nonlocal diffusion problems, Archive for Rational Mechanics and Analysis, vol. 187, no. 1, pp. 137–156, 2008.
[20] B. Alali and M. Gunzburger, Peridynamics and material interfaces, Journal of Elasticity, vol. 120, no. 2, pp. 225–248, 2015.
[21] E. Aulisa, G. Capodaglio, A. Chierici, and M. D'Elia, Efficient quadrature rules for finite element discretizations of nonlocal equations, Numerical Methods for Partial Differential Equations, pp. 1–27, 2021.
[22] V. Girault and P.-A. Raviart, Finite element methods for Navier-Stokes equations: theory and algorithms, vol. 5. Springer Science & Business Media, 2012.
[23] M. D. Gunzburger and L. S. Hou, Finite–dimensional approximation of a class of constrained nonlinear optimal control problems, SIAM Journal on Control and Optimization, vol. 34, no. 3, pp. 1001–1043, 1996.
[24] F. Trøltzsch, Optimal control of partial differential equations: theory, methods, and applications, vol. 112. American Mathematical Society, 2010.
[25] M. Bergounioux, K. Ito, and K. Kunisch, Primal-dual strategy for constrained optimal control problems, SIAM Journal on Control and Optimization, vol. 37, no. 4, pp. 1176–1194, 1999.

Department of Mathematics and Statistics, Texas Tech University, Lubbock, TX 79409
E-mail: giorgio.bornia@ttu.edu

Department of Industrial Engineering, Lab. of Montecuccolino, University of Bologna, Via dei Colli 16, 40136 Bologna, Italy
E-mail: andrea.chierici4@unibo.it

School of Informatics, Computing, and Cyber Systems, Northern Arizona University, S. San Francisco Street, Flagstaff, AZ 86011
E-mail: saikanth.ratnavale@nau.edu